SEMIANNUAL REPORT

CFD CODE EVALUATION

NAG8–095

(April 1988 – September 1988)

T. J. Chung, Y. M. Kim, and R. Hallit

Department of Mechanical Engineering
The University of Alabama in Huntsville
Huntsville, AL 35899

prepared for

NASA/MSFC

October, 1988

TABLE OF CONTENTS

SUMMARY

The task carried out under this research grant covers research on accuracy and efficiency of CFD strategies, error estimates for convective terms, and antidiffusion. These basic studies (see Appendices A through C) are considered important in evaluating available CFD codes which will be the main activities for the next year.

APPENDIX A

CONVERGENCE STUDIES FOR CONVECTIVE TERMS

Given: Burgers equation, geometry as shown in Fig. A.1.

$$\frac{\partial u}{\partial t} + u\frac{\partial u}{\partial x} + v\frac{\partial v}{\partial x} - \nu\left[\frac{\partial^2 u}{\partial x^2} + \frac{\partial^2 u}{\partial y^2}\right] - f_x = 0$$

$$\frac{\partial v}{\partial t} + u\frac{\partial v}{\partial x} + v\frac{\partial v}{\partial y} - \nu\left[\frac{\partial^2 v}{\partial x^2} + \frac{\partial^2 v}{\partial y^2}\right] - f_y = 0$$

$$f_x = \frac{1}{1+t}\left[x^2 + 2xy - \frac{1}{1+t}\right] + 3x^3y^2 - 2\nu y$$

$$f_y = \frac{1}{1+t}\left[y^2 + 2xy - \frac{1}{1+t}\right] + 3x^2y^3 - 2\nu x$$

Exact Solution:

$$u = \frac{1}{1+t} + x^2y$$

$$v = \frac{1}{1+t} + xy^2$$

Required:

With SUPG, Newton–Raphson iterations, and bilinear isoparametric elements, the coarse, intermediate and fine mesh shown in Fig. A1. Use $\nu = 1$ and $\nu = 10^6$; $\Delta t = 10^{-6}$, 10^{-4}, 10^{-2}, 1, 10^2; $\eta = 0, 1/2, 1$.

Solution:

The RMS errors vs Δt in log scales shown in Figs. A.1 and A.2 have trends similar to the linear problem (without convection terms) The error increases monotonically with an increase of Δt for $\eta = 1/2$, whereas the error is almost independent of Δt for $\eta = 1$. The results for $\eta = 0$ are not presented as they are outside of the scale shown. If $\nu = 1$, the error increases as Δt becomes small due to round-off errors. The error decreases rapidly as the mesh is refined.

Remarks

The Newton–Raphson scheme converges after 4 or 5 iterations. It should be noted that the combination of the SUPG and Newton–Raphson procedures are responsible for a stable and accurate solution.

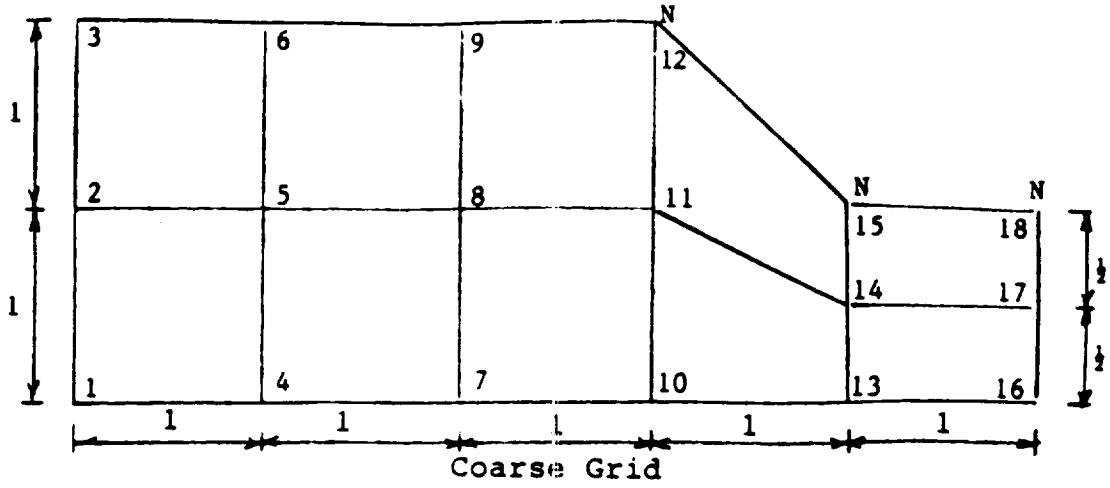

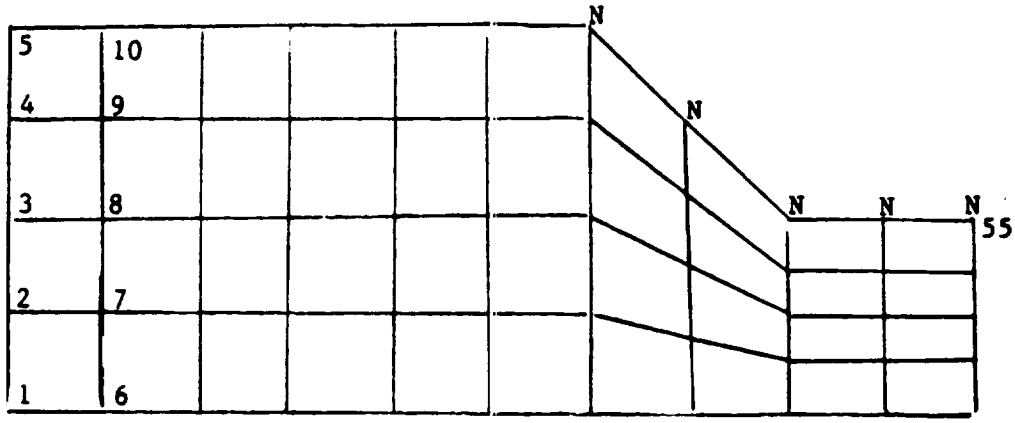

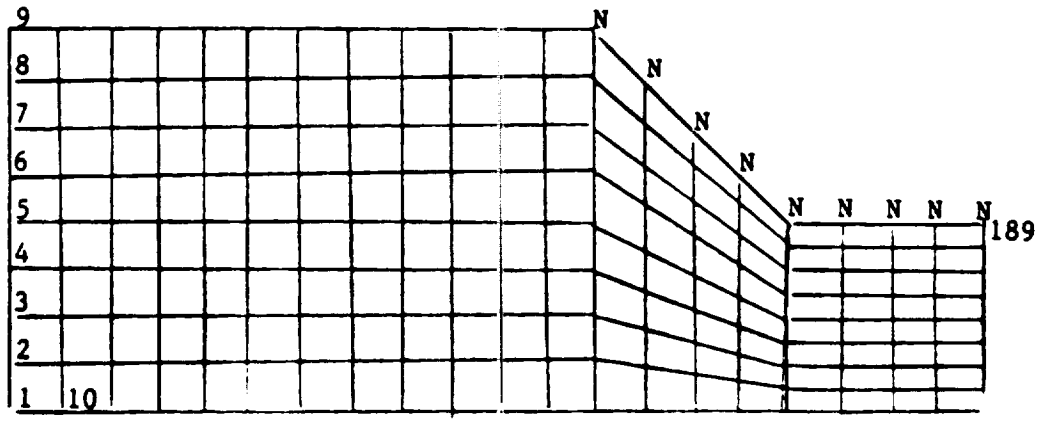

Note: N represents Neumann boundary conditions. For example, at node 12 for Coarse Grids $\frac{\partial u}{\partial x} = 2xy$, $\frac{\partial u}{\partial y} = x^2$, $\frac{\partial v}{\partial x} = y^2$, $\frac{\partial v}{\partial y} = 2xy$ are prescribed. Dirichlet boundary conditions are prescribed for all other boundary nodes from the exact solution.

Use u=v=0 as the initial guess for all interior nodes.

Fig. A.1 Geometries for Example 6.4.1.

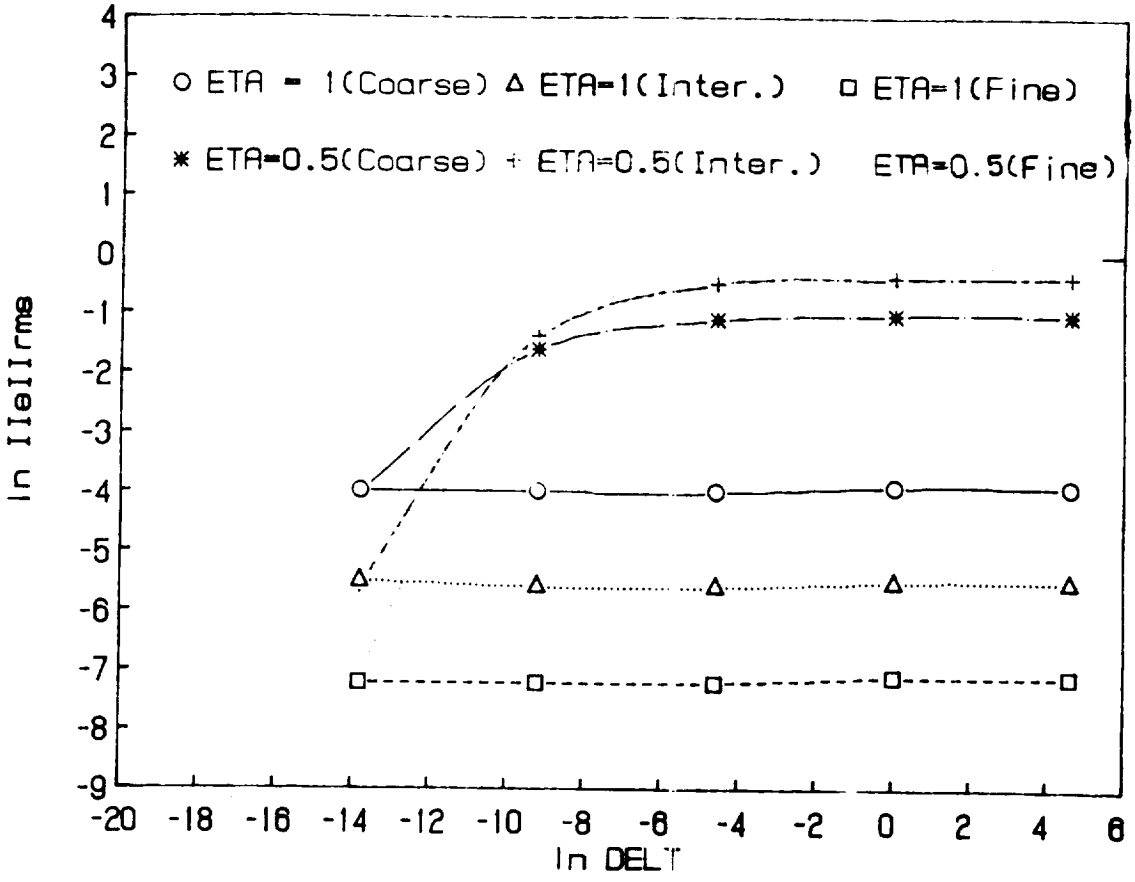

Fig. A.2 RMS error for Example 6.4.1, $\nu = 10^6$.

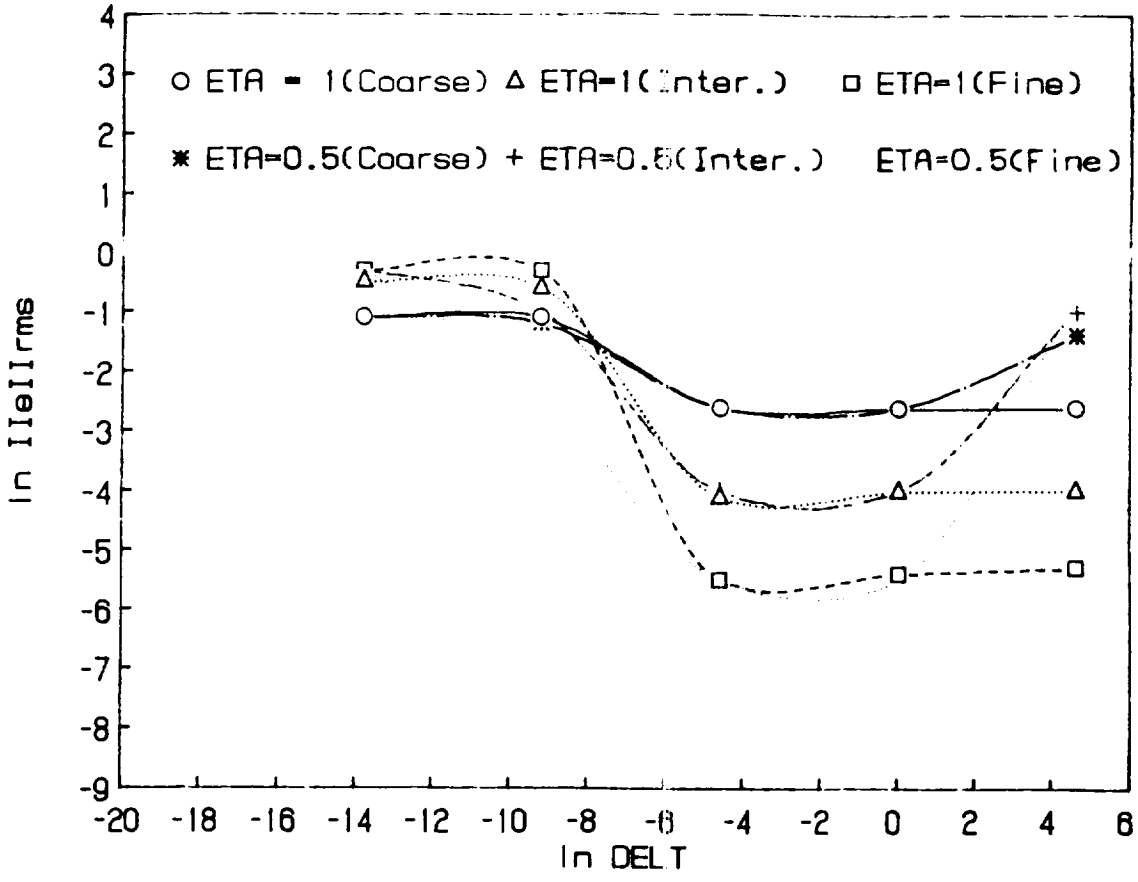

Fig. A.3 RMS error for Example 6.4.2, $\nu = 1$.

APPENDIX B

ERROR ESTIMATES FOR CONVECTIVE TERMS

The standard Galerkin finite element method is known to have computational instabilities in the convection dominated flow field. To overcome difficulties involved in the convective nature of hyperbolic equations, the SUPG scheme may be used. The error estimates will be discussed for the cases with and without diffusion terms.

Consider the convection equation of the form

$$Lu = f \qquad \text{in } \Omega \tag{B.1a}$$

$$u = g \qquad \text{on } \Gamma \tag{B.1b}$$

with

$$L = a_i(\mathbf{x}) \frac{\partial}{\partial x_i}$$

The inner product of (B.1a) and the test function including the sum of the trial functions and the numerical diffusion test functions leads to the problem: Find $\tilde{u} \in S_h$ such that

$$\begin{aligned}[((\mathbf{a} \cdot \nabla)\tilde{u},v) + h(\mathbf{a} \cdot \nabla)v] - (1 + h)(\tilde{u},v) \\ = (f, v + h(\mathbf{a} \cdot \nabla)v) - (1 + h)(g,v) \qquad \forall\, v \in S_h\end{aligned} \tag{B.2}$$

Then there exists constant c if $\tilde{u}$ satisfies (B.2) such that

$$\|u - \tilde{u}\|_{L_2(\Omega)} \le c h^{k+1/2} \|u\|_{H^{r+1}} \tag{B.3}$$

To prove this, let $\tilde{u}^h \in S_h$ be an interpolant of u satisfying the steady–state case. Denoting $e^h = u - \tilde{u}^h$ and $\tilde{e}^h = \tilde{u} - \tilde{u}^h$, we obtain [Johnson, 1988]

$$\begin{aligned}\|e\|^2_{L_2(\Omega)} &= B(e,e) = B(e,e^h) - B(e,\tilde{e}^h) = B(e,e^h) \\ &= ((\mathbf{a} \cdot \nabla)e,e^h) + h((\mathbf{a} \cdot \nabla)e,\tilde{e}^h) + (e,e^h) \\ &+ h(e,(\mathbf{a} \cdot \nabla)e^h) - (1 + h)(e,e^h) \\ &\le \frac{h}{4} \|(\mathbf{a} \cdot \nabla)e\|^2 + h^{-1}\|e^h\|^2 + \frac{h}{4} \|(\mathbf{a} \cdot \nabla)e\|^2 \\ &+ h\|(\mathbf{a} \cdot \nabla)e^h\|^2 + \frac{1}{4} \|e\|^2 + \|e^h\|^2 \\ &+ \frac{1}{4} \|e\|^2 + h^2\|(\mathbf{a} \cdot \nabla)e^h\|^2 + \frac{1 + h}{4} |e|^2 + (1 + h)|e^h|^2\end{aligned} \tag{B.4}$$

We consider the inequality

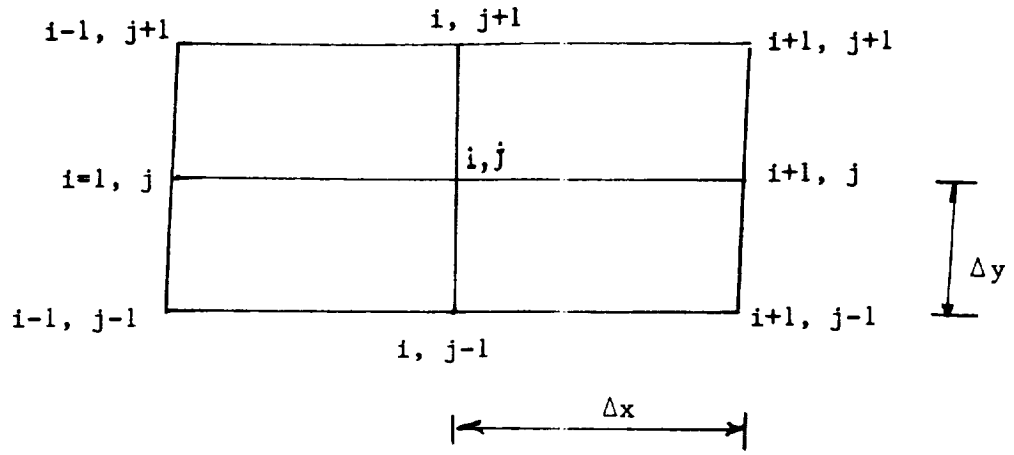

(a)

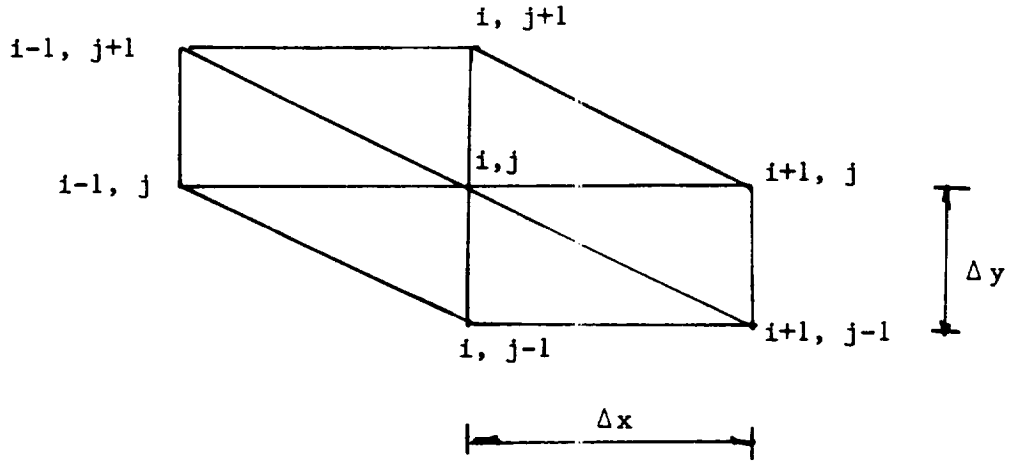

(b)

Fig. B.1 Typical interior nodes of (a) quadrilateral mesh and (b) triangular mesh for stability analysis.

$$2ab \leq \epsilon a^2 + \epsilon^{-1} b^2 \tag{B.5}$$

which may be used in (B.4) so that

$$\|e\|^2_{L_2(\Omega)} \leq ch^{2k+1} \|u\|^2_{H^{k+1}(\Omega)} \tag{B.6}$$

or

$$\|e\|_{L_2(\Omega)} \leq ch^{k+1/2} \|u\|_{H^{k+1}(\Omega)} \tag{B.7}$$

If the standard Galerkin method is used, then we have

$$\begin{aligned} \|e\|^2_{L_2(\Omega)} &= ((\mathbf{a} \cdot \nabla) e^h, \tilde{e}^h) + (e^h, \tilde{e}^h) - (e^h, \tilde{e}^h) \\ &\leq \|(\mathbf{a} \cdot \nabla) e^h\|^2 + \|e^h\|^2 + \frac{1}{2} \|\tilde{e}^h\| + \|e^h\|^2 + \frac{1}{4} |\tilde{e}^h|^2 \end{aligned} \tag{B.8}$$

or

$$\|e\|_{L_2(\Omega)} \leq ch^k \|u\|_{H^{k+1}(\Omega)} \tag{B.9}$$

Comparing (B.7) and (B.9), it is seen that the SUPG approximation provides $O(h^{\frac{1}{2}})$ larger than the standard Galerkin approximation Experience has shown that, in the standard Galerkin methods, oscillations propagate in the crosswind and in the upwind directions with little damping, whereas such oscillations decay rapidly in both directions.

The error estimates for the steady state convection–diffusion equation are evaluated in a manner similar to the convection equation. Consider the governing equation in the form

$$Lu - \nabla^2 u = f \qquad \text{in } \Omega \tag{B.10a}$$

$$u = g \qquad \text{on } \Gamma \tag{B.10b}$$

In view of the steady–state results and from the analysis carried out for the convection equation, we obtain

$$\|e\|_{L_2(\Omega)} \leq ch^{k+1/2} \|u\|_{H^{k+1}(\Omega)} \tag{B.11}$$

which is identical to (B.7).

The mathematical justification for the gradient discontinuity test function has not

been studied in detail. This question remaint largely empirical until further investigations are carried out.

The error estimates for the unsteady streamline diffusion method require the analysis of the step in (B.7). Thus,

$$\|\epsilon(t)\| \le c_1 h^{k+1/2} \|u\|_{H^{k+1}(\Omega)} + c_2 h^k \int_0^{n\Delta t} \|u\|_{H^{k+1}(\Omega)} dt \tag{B.12}$$

It should be noted that for each time step n, the analysis indicated in (B.12) is linear, but the solution u^n will, in general, have jumps across the discrete time levels t_n.

We have discussed the error estimates as the convergence to the exact solution is being pursued. It has been shown that these error estimates are defined in various norms. Accuracy may be sought as high as desired by refining the computational mesh. However, the transient solutions are affected greatly by certain combinations of mesh sizes and temporal increments. It is well known that computational instability arises or amplitudes grow without bound if stability conditions are not met. Toward this end, we shall examine the so–called von Neumann stability analysis.

Consider the convection equation

$$\frac{\partial u}{\partial t} = a \frac{\partial u}{\partial x}$$

The corresponding Taylor–Galerkin scheme can be written as

$$\left[\int_\Omega \left[\Phi_\alpha \Phi_\beta + \frac{a^2 \Delta t^2}{6} \frac{\partial \Phi_\alpha}{\partial x} \frac{\partial \Phi_\beta}{\partial x}\right] d\Omega\right] \frac{v_\beta^{n+1}}{\Delta t} = a \int_\Omega \Phi_\alpha \frac{\partial u^n}{\partial x} d\Omega - \frac{a^2 \Delta t}{2} \int_\Omega \frac{\partial \Phi_\alpha}{\partial x} \frac{\partial u^n}{\partial x} d\Omega$$
$$+ \frac{a^2 \Delta t}{6} \left[\int_\Gamma \Phi_\alpha \frac{\partial v^{n+1}}{\partial x} d\Gamma\right] + \frac{a^2 \Delta t}{2} \left[\int_\Gamma \Phi_\alpha \frac{\partial u^n}{\partial x} d\Gamma\right] \tag{B.13}$$

where $v^{n+1} = u^{n+1} - u^n$.

For a linear element with a uniform grid, the global finite element equation at the node j takes the form

$$\frac{1}{\Delta t}\left[\frac{1}{6} v_{j-1} + \frac{2}{3} v_j + \frac{1}{6} v_{j+1}\right] - \frac{a^2 \Delta t}{6}\left[\frac{v_{j-1} - 2v_j + v_{j+1}}{\Delta x^2}\right]$$
$$= a\left[\frac{u_{j+1} - u_{j-1}}{2\Delta x}\right] + \frac{a^2 \Delta t}{2}\left[\frac{u_{j-1} - 2u_j + u_{j+1}}{\Delta x^2}\right]$$

which may be simplified as

$$v_j^{n+1} + \frac{1}{6}(v_{j-1}^{n+1} - 2v_j^{n+1} + v_{j+1}^{n+1}) - \frac{1}{6}\left[\frac{a\Delta t}{\Delta x}\right]^2(v_{j-1}^{n+1} - 2v_j^{n+1} + v_{j+1}^{n+1})$$
$$= \left[\frac{a\Delta t}{\Delta x}\right]\frac{(u_{j+1}^n - u_{j-1}^n)}{2} + \frac{1}{2}\left[\frac{a\Delta t}{\Delta x}\right]^2(u_{j-1}^n - 2u_j^n + u_{j+1}^n)$$

or

$$v_j^{n+1} + \frac{1}{6}(1-c^2)\delta^2 v_j^{n+1} = c\Delta_0 u_j^n + \frac{1}{2}c^2\delta^2 u_j^n\left[1 + \frac{1}{6}(1-c^2)\delta^2\right](u_j^{n+1} - u_j^n)$$
$$= c\Delta_0 u_j^n + \frac{1}{2}c^2\delta^2 u_j^n \qquad \text{(B.15)}$$

where $\Delta_0 u_j = (1/2)(u_{j+1} - u_{j-1})$, $\delta^2 u_j = u_{j+1} - 2u_j + u_{j-1}$, and $c = a\Delta t/\Delta x$ (Courant number). The combined spatial and temporal response of the amplitude may be written as

$$u_j^n = e^{i\beta x}e^{\alpha t} = e^{i\beta jh}e^{\alpha nk} = e^{i\beta jh}g^n \qquad \text{(B.16)}$$

where $g = e^{\alpha k}$ (amplification factor), $h = \Delta x$, $k = \Delta t$, α = constant, β = constant determined by initial condition, and

$$v_j^{n+1} = u_j^{n+1} - u_j^n = e^{i\beta jh}(g-1)g^n \qquad \text{(B.17)}$$

Substituting (B.16) and (B.17) into (B.15) yields

$$e^{i\beta jh}(g-1)g^n + \frac{1}{6}(1-c^2)(g-1)g^n e^{i\beta(j-1)h}(1 - 2e^{i\beta h} + e^{2i\beta h})$$

or

$$(g-1)\left[1 + \frac{1}{6}(1-c^2)(e^{-i\beta h} - 2 + e^{i\beta h})\right]$$
$$= \frac{1}{2}c(e^{i\beta h} - e^{-i\beta h}) + \frac{1}{2}c^2(e^{-i\beta h} - 2 + e^{i\beta h}) \qquad \text{(B.18)}$$

Denoting $\eta = \beta h$ and using the trigonometric relations, it follows from (B.18) that

$$g = 1 + \left[1 - \frac{2}{3}(1-c^2)\sin^2\frac{1}{2}\eta\right]^{-1}\left[ic\sin\eta - 2c^2\sin^2\frac{1}{2}\eta\right] \qquad \text{(B.19)}$$

Notice that as $\eta \to 0$, Eq. (B.19) reduces to

$$g = 1 + ic\eta - \frac{1}{2}c^2\eta^2 - \frac{1}{6}ic^3\eta^3 + O(\eta^4) \qquad \text{(B.20)}$$

It is clear that the stability condition requ res $c \leq 1$, which provides $|g| \leq 1$ for $c = 1$. This implies that signals are propagated without distortion when the characteristics pass through the nodes.

Using a similar approach, it can be shown that, for two–dimensional quadrilateral elements, the amplification factor at an interior node becomes (Fig. B.1a)

$$g = 1 - 2c_x^2 \sin^2 \frac{k_x \Delta x}{2} \cos^2 \frac{k_y \Delta y}{2} - 2c_y^2 \sin^2 \frac{k_y \Delta y}{2} \cos^2 \frac{k_x \Delta x}{2}$$
$$- c_x c_y \sin k_x \Delta x \sin k_y \Delta y - i\left[c_x \sin k_x \Delta x \cos^2 \frac{k_y \Delta y}{2}\right.$$
$$\left. + c_y \sin k_y \Delta y \cos^2 \frac{k_x \Delta x}{2}\right] \tag{B.21}$$

where k_x and k_y are the wave numbers of the Fourier components, c_x and c_y are the Coant numbers in the coordinate directions, and Δx and Δy are the mesh spacings.

The amplification factor for an interior node of a typical triangular element assumes the form (Fig. B.1b)

$$g = 1 - 2c_x^2 \sin^2 \frac{k_x \Delta x}{2} - 2c_y^2 \sin^2 \frac{k_y \Delta x}{2} + c_x c_y [\cos k_x \Delta x$$
$$+ \cos k_y \Delta y - \cos(k_x \Delta x - k_y \Delta y)] - i\left\{\frac{c_x}{3} [\sin k_y \Delta x\right.$$
$$+ \sin(k_x \Delta x - k_y \Delta y)] + \frac{c_y}{3} [\sin k_x \Delta x + 2 \sin k_y \Delta y$$
$$\left. - \sin(k_x \Delta x - k_y \Delta y)]\right\} \tag{B.22}$$

Now, consider a mesh with $\Delta x = \Delta y$ and waves $k_x = k_y$, Courant numbers $c_x = c_y$. The stability limits for quadrilateral and triangular meshes are $c < 1$ and $c < 1/2$, respectively.

Let us now examine the advection–diffusion

$$u_t = -a u_x + \nu v_{xx} \tag{B.23}$$

$$\frac{1}{\Delta t}\left[\frac{1}{6} v_{j-1} + \frac{2}{3} v_j + \frac{1}{6} v_{j+1}\right] + \frac{a}{2}\left[\frac{v_{j+1} - v_{j-1}}{2\Delta x}\right] - \left[\frac{v_{j-1} - 2v_j + v_{j+1}}{\Delta x^2}\right]$$

$$= -a\left[\frac{u_{j+1} - u_{j-1}}{2\Delta x}\right] + \nu\left[\frac{u_{j-1} - 2u_j + u_{j+1}}{\Delta x^2}\right]$$

Denoting $d = \nu\Delta t/h^2$, Eq. (B.24) becomes

$$v_j + \frac{1}{6}(v_{j-1} - 2v_j + v_{j+1}) + \frac{1}{2}\frac{a\Delta t}{\Delta x}\left[\frac{v_{j+1} - v_{j-1}}{2}\right] - \frac{1}{2}\frac{\nu\Delta t}{\Delta x^2}(v_{j-1} - 2v_j + v_{j+1})$$

$$= \frac{a\Delta t}{\Delta x}\left[\frac{u_{j+1} - u_{j-1}}{2}\right] + \frac{\nu\Delta t}{\Delta x^2}(u_{j-1} - 2u_j + u_{j+1})$$

or

$$v_j + \frac{1}{6}\delta^2 v_j + \frac{1}{2}c\Delta_0 v_j - \frac{1}{2}d\delta^2 v_j = -c\Delta_0 u_j - d\delta^2 u_j\left[1 + \frac{1}{6}\delta^2 -\right.$$

$$\left. - \frac{1}{2}(-c\Delta_0 + d\delta^2)\right](u_j^{n+1} - u_j^n) = (-c\Delta_0 + d\delta^2)u_j^n \qquad \text{(B.25)}$$

The necessary and sufficient condition for stability according to Lax–Richtmyer [1968]

$$\text{if} \quad \frac{\partial u}{\partial t} \le 0, \qquad |g| \le 1 \qquad \text{(B.26)}$$

$$\text{if} \quad \frac{\partial u}{\partial t} > 0, \qquad |g| \le 1 + O(k) \qquad \text{(B.27)}$$

Proceeding in a manner similar to the case of the convection equation, Eq. (B.25) reduces to

$$e^{i\beta jh}(g-1)g^n + \frac{1}{6}(g-1)g^n e^{i\beta(j-1)h}(1 - 2e^{i\beta h} + e^{2i\beta h})$$
$$+ \frac{1}{4}c(g-1)g^n e^{i\beta(j-1)h}(e^{2i\beta h} - 1) - \frac{1}{2}d(g-1)g^n e^{i\beta(j-1)h}(1 - 2e^{i\beta h} + e^{2i\beta h})$$
$$= -\frac{1}{2}cg^n e^{i\beta(j-1)h}(e^{2i\beta h} - 1) + dg^n e^{i\beta(j-1)h}(1 - 2e^{i\beta h} + e^{2i\beta h}) \qquad \text{(B.28)}$$

or

$$g^n(g-1)e^{i\beta h} + \frac{1}{6}(g-1)g^n(1 - 2e^{i\beta h} + e^{2i\beta h})$$
$$+ \frac{1}{4}c(g-1)g^n(e^{2i\beta h} - 1) - \frac{d}{2}(g-1)g^n(1 - 2e^{i\beta h} + e^{2i\beta h})$$
$$= -\frac{1}{2}cg^n(e^{2i\beta h} - 1) + dg^n(1 - 2e^{i\beta h} + e^{2i\beta h}) \qquad \text{(B.29)}$$

Further simplifications of (B.29) result in

$$g = 1 + \left[1 + \left[\frac{1}{3} - d\right](\cos\beta h - 1) + \frac{1}{2}ic\sin\beta h\right]^{-1}[-ic\sin\beta h + 2d(\cos\beta h - 1)] \qquad \text{(B.30)}$$

or

$$g - 1 = \frac{\left[-ic \sin^{\eta\eta\alpha} - 4d\sin^2 \frac{\eta}{2}\right]}{\left[1 - 2\left[\frac{1}{3} - d\right]\sin^2 \frac{\eta}{2} + \frac{1}{2} ic \sin\eta\right]} \tag{B.31}$$

Finally, as $\eta \to 0$, we arrive at

$$g = 1 - ic\eta - \left[d + \frac{1}{2}c^2\right]\eta^2 + ic\left[d + \frac{1}{4}c^2 - \frac{1}{6}\right]\eta^3 + \ldots \tag{B.32}$$

In comparison with (B.20), the stability criterion as given by (B.32) represents greater stability apparently due to the presence of physical viscosity.

APPENDIX C

ANTIDIFFUSION

With all the schemes devised in the previous discussions, difficulties involved in steep gradients and widely disparate time and length scales may still persist. The FCT method originally proposed by Boris and Book [1973] and subsequently extended to the multidimensional case by Zalesak [1979] has been applied to the high–speed compressible flow problems in the context of finite elements [Erlebacher, 1984; Parrot and Christie, 1986; Löhner, et al, 1986].

The FCT method is to combine the high–order scheme which may cause over–shooting with the lower–order scheme to stabilize through appropriate limiting processes. The high–order scheme may be generated from GGFE, whereas the low order scheme is equivalent to the SD–GGFE method which is specifically designed to stabilize the convective terms. Thus, the combination of FCT and SD–GGFE should enhance the desirability of both methods.

The high–order scheme may follow the Standard Taylor–Galerkin process, or more preferably GGFE without SUPG in the present context. We write

$$A_{\alpha\beta}\frac{\Delta U_\beta^{(1)}}{\Delta t} = -\frac{1}{2}\left[B^s_{\alpha\beta}(F^{n+1}_{\beta j} - F^n_{\beta j}) - K_{\alpha\beta}\,(G^{n+1}_{\beta j} - G^n_{\beta j})\right] + H^n_\alpha + N_\alpha \qquad (C.1)$$

which corresponds to step 1 given by (5.3.1), with step 2 (5.3.2) vanishing. For this problem, therefore, we must modify the approach as follows: Let $\Delta U_\beta^{(1)} / \Delta t$ in (C.1) be defined between the time steps n and $n+\frac{1}{2}$ and write for each element,

$$a_e U_e^{n+\frac{1}{2}} = A_N U^n_{N_e} + \frac{\Delta t}{2} B^s_N F^n_{N_e} + H^n_e \qquad (C.2)$$

where a_e is the area of each local element,

$$a_e = \int_{\Omega e} d\Omega\,, \qquad A_N = \int_{\Omega e} \Phi^{(e)}_N \, d\Omega\,, \qquad H^s_N = \int_{\Omega e} \Phi^{(e)}_{N,j} \, d\Omega \qquad (C.3)$$

where N represents the local node. The right–hand side of (C.2) can be evaluated locally

and summed through the local nodes for each element. No boundary conditions need be imposed at this stage. The initial guess for all variables is required to solve (C.2).

The next step is to rewrite (C.1) in the form:

$$A_{\alpha\beta}U_{\beta}^{n+1} = A_{\alpha\beta}U_{\beta}^{n+\frac{1}{2}} + \Delta t(B_{\alpha\beta}F_{\beta j}^{n+\frac{1}{2}} + K_{\alpha\beta}G_{\beta j}^{n+\frac{1}{2}} + H_{\alpha}^{n+\frac{1}{2}} + N_{\alpha}) \tag{C.4}$$

where $B_{\alpha\beta}$ is the convection matrix with only the standard test function and $F_{\beta j}^{n+\frac{1}{2}}$, $G_{\beta j}^{n+\frac{1}{2}}$, and $H_{\alpha}^{n+\frac{1}{2}}$ are still the same as in the time step n but will be updated as the next time step is incremented. The process characterized by (C.4) is seen to be equivalent to the classical Lax–Wendroff method. The solution of (C.4) may require several iterative cycles within each time increment by introducing the lumped mass matrix

$$A_{\alpha\beta}^{(L)}\Delta U_{\beta}^{r+1} = E_{\alpha j}^{r} - A_{\alpha\beta}^{(C)}\Delta U_{\beta}^{r} \tag{C.5}$$

where $E_{\alpha j}^{r}$ represents the terms on the right–hand side of (C.4) except for the first term. The solution of (C.5) is referred to as the high–order scheme.

The low–order scheme is devised in order to obtain monotonic results. This can be achieved by adding artificial viscosity such as that of Lapidus and Pinder [1982]. However, the SDM–GGFE scheme can be employed. This will require the numerical diffusion matrix $C_{\alpha\beta}$ and the gradient discontinuity matrix $D_{\alpha\beta}$ which will be added to $B_{\alpha\beta}$ associated with $F_{\beta j}$ in (C.4).

$$A_{\alpha\beta}\Delta U_{\beta}^{n+1} = \Delta t\left[(B_{\alpha\beta} + C_{\alpha\beta} + D_{\alpha\beta})\, F_{\beta j}^{n+\frac{1}{2}} + K_{\alpha\beta}G_{\beta j}^{n+\frac{1}{2}} + H_{\alpha}^{n+\frac{1}{2}} + N_{\alpha}\right]$$

or

$$A_{\alpha\beta}\Delta U_{\beta}^{n+1} = W_{\alpha j}^{n+\frac{1}{2}} + E_{\alpha j}^{n+\frac{1}{2}} \tag{C.6}$$

with

$$E_{\alpha j}^{n+\frac{1}{2}} = (C_{\alpha\beta} + D_{\alpha\beta})\, F_{\beta j}^{n+\frac{1}{2}} \tag{C.7}$$

where $E_{\alpha j}^{n+\frac{1}{2}} = (C_{\alpha\beta} + D_{\alpha\beta})F_{\beta j}^{n+\frac{1}{2}}$. The low–order scheme is then implemented through a lumped mass matrix $A_{\alpha\beta}^{(L)}$ which would enhance the diffusive effect.

$$A_{\alpha\beta}^{(L)}\Delta U_{\beta}^{\ell} = W_{\alpha j} + E_{\alpha j} \tag{C.8}$$

with ℓ denoting the low–order scheme.

Since the higher–order scheme is considered as underdiffused whereas the low–order scheme is overdiffused, it is necessary that we seek an optimum. To this end, subtracting (C.8) from (C.5) yields

$$A_{\alpha\beta}(\Delta U_\beta^h - \Delta U_\beta^\ell) = (A_{\alpha\beta}^{(L)} - A_{\alpha\beta}^{(C)})\,\Delta U_\beta^h - F_{\alpha j} \tag{C.9}$$

with h denoting the high–order scheme (C.5). Here, it is seen that an appropriate limiting or antidiffuse process for $(\Delta U_\beta^h - \Delta U_\beta^\ell)$ would be crucial To prevent undershoots or overshoots. The combined high and low–order schemes may be written as

$$U_\alpha^{n+1} = U_\alpha^n + U_\alpha^\ell + (\Delta U_\alpha^h - \Delta U_\alpha^\ell)$$

or

$$\Delta U_\alpha^{n+1} = U_\alpha^\ell + \eta \Delta \overline{U}_\alpha \tag{C.10}$$

where η is the limiting parameter with the ranges

$$-1 < \eta < 1 \tag{C.11}$$

$$U_\alpha^\ell = U_\alpha^n + U_\alpha^\ell \tag{C.12}$$

$$\Delta \overline{U}_\alpha = \Delta U_\alpha^h - \Delta U_\alpha^\ell \tag{C.13}$$

Here, the limiting process must be carried out at the element level in order to ensure local conservation requirements by means of the limiting parameter η. The magnitude and sign of the limiting parameter η can be determined as follows:

(1) To determine the nodal values in the form of

$$U_\alpha^{n+1} = U_\alpha^\ell + \sum_{e=1}^{E} (\eta_e \Delta \overline{U}_e) \tag{C.14}$$

(2) First determine η_e

$$\eta_e = \min \begin{cases} R^+ & \text{if } \eta_e \Delta \overline{U}_e > 0 \\ R^- & \text{if } \eta_e \Delta U_e < 0 \end{cases} \tag{C.15}$$

where

$$R_-^+ = \begin{cases} \min\,(1, Q_-^+ / p_-^+) & \text{if} \quad p^+ > 0,\ p^- < 0 \\ 0 & \text{if} \quad p_-^+ = 0 \end{cases} \tag{C.16}$$

where p^{+}_{-} is the sum of all positive (negative) antidiffuse element contributions to node α,

$$p^{+}_{-} = \sum_{e=1}^{E} \left\{ \begin{matrix} \max \\ \min \end{matrix} \right\} (0 , \eta_e) \tag{C.17}$$

and Q^{+}_{-} is the maximum (minimum) increment (decrement) node α allowed to achieve in (C.4),

$$Q^{+}_{-\alpha} = U_{\alpha}^{\begin{matrix} \min \\ \max \end{matrix}} - U^{\ell}_{\alpha} \tag{C.18}$$

where $U_{\alpha}^{\begin{matrix} \min \\ \max \end{matrix}}$ can be determined as follows:

(1) Maximum (minimum) nodal values U^{n}_{α}

$$U_{\alpha} = \left\{ \begin{matrix} \max \\ \min \end{matrix} \right\} (U^{\ell}_{\alpha} , U^{n}_{\alpha}) \tag{C.19}$$

(2) Maximum (minimum) nodal values of element

$$U_e = \left\{ \begin{matrix} \max \\ \min \end{matrix} \right\} (U_1, U_2, U_3,\ldots U_N) \tag{C.20}$$

where 1,2,3...N represent the nodes of element e

(3) Maximum (minimum) U_e of all elements surrounding node α

$$U_{\alpha}^{\begin{matrix} \max \\ \min \end{matrix}} = \left\{ \begin{matrix} \max \\ \min \end{matrix} \right\} (U_1, U_2, U_3, \ldots U_M) \tag{C.21}$$

where 1,2,3, ... M represent the elements surrounding node α.

With (C.21) substituted into (C.18) and subsequently to (C.16), (C.15), (C.14), and finally to (C.10), we complete the limiting process.

In summary, the limiting process should generate no new maxima and minima in the solution, nor should it accentuate already existing extrema. Such a prescription obviously maintains positivity. To this end, we must correct the antidiffuse mass fluxes. Note that the antidiffuse fluxes are limited term by term so that antidiffuse flux transfer can push the flux value at any node beyond the flux value at neighboring nodes. This is the origin of the name Flux Corrected Transport [Boris and Book, 1971].

The limiting process described above may be applied to a single variable. Density is the most logical choice in compressible flows. Although, this will reduce the amount of computing time, adequacy of involving other variables also should be verified in each

problem under study. Furthermore, the most acceptable limiting procedure for antidif-
fussion remains an open question, subject to extensive future research.